European Journal of Medicinal Chemistry 82 (2014) 536–544

Contents lists available at ScienceDirect

European Journal of Medicinal Chemistry

journal homepage: http://www.elsevier.com/locate/ejmech

Original article

Synthesis and anti-cholinesterase activity of new 7-hydroxycoumarin derivatives

Masoumeh Alipour [a], Mehdi Khoobi [a], Alireza Moradi [b], Hamid Nadri [b], Farshad Homayouni Moghadam [c], Saeed Emami [d], Zeinab Hasanpour [a], Alireza Foroumadi [a], Abbas Shafiee [a, *]

[a] Department of Medicinal Chemistry, Faculty of Pharmacy and Pharmaceutical Sciences Research Center, Tehran University of Medical Sciences, Tehran 14176, Iran
[b] Faculty of Pharmacy, Shahid Sadoughi University of Medical Sciences, Yazd, Iran
[c] Neurobiomedical Research Center, School of Medicine, Shahid Sadoughi University of Medical Sciences, Yazd, Iran
[d] Department of Medicinal Chemistry and Pharmaceutical Sciences Research Center, Faculty of Pharmacy, Mazandaran University of Medical Sciences, Sari, Iran

ARTICLE INFO

Article history:
Received 15 February 2014
Received in revised form
18 May 2014
Accepted 23 May 2014
Available online xxx

Keywords:
Alzheimer's disease
Acetylcholinesterase
Coumarins
Docking study

ABSTRACT

A series of 7-hydroxycoumarin derivatives connected by an amidic linker to the different amines were designed and synthesized as cholinesterase inhibitors. Most compounds showed remarkable inhibitory activity against acetylcholinesterase (AChE) and butyrylcholinesterase (BuChE). Among them, *N*-(1-benzylpiperidin-4-yl)acetamide derivative **4r** with IC_{50} value of 1.6 μM was the most potent compound against AChE. The selectivity index of compound **4r** for anti-AChE activity was about 26. Moreover, the compound **4r** significantly protected PC12 neurons against H_2O_2-induced cell death at low concentrations. The docking study of compound **4r** with AChE enzyme showed that both CAS and PAS are occupied by the ligand.

1. Introduction

Alzheimer's disease (AD) is a progressive neurodegenerative disorder characterized by cognitive impairment, loss of memory and language deterioration [1]. It is the most common form of dementia affecting more than 5% of the population over the age of 65 years [2].

At the molecular level, patients affected by AD show abnormal deposits of β-amyloid peptide (Aβ) and abnormal spiral filaments in neurons, increased oxidative stress, and low levels of acetylcholine (ACh) [3]. In general, the death of neurons during the progression of AD affects the levels of brain neurotransmitters. Besides ACh, other neurotransmitter, e.g. glutamate and serotonin are also affected later in the disease [4].

Currently, there is no cure for AD and treatment strategies being primarily symptomatic. The main therapeutic strategy is based on the cholinergic hypothesis and specifically on acetylcholinesterase (AChE) inhibition to improve cholinergic neurotransmission in the brain [5]. The recent studies have shown that AChE involves in the extraneous non-cholinergic function by binding to Aβ [6,7]. The X-ray crystallography of AChE structure has demonstrated that the active site of AChE is a deep and narrow gorge mainly composed of two distinct binding sites: the Ser-His-Glu catalytic site located at the bottom of gorge, and the peripheral anionic binding site (PAS) located at the gorge entrance [8]. The PAS has a crucial role in the polymerization of Aβ plaques and fibrils formation [9].

In the recent decades, several AChE inhibitors such as donepezil, tacrine, rivastigmine, and galantamine have been introduced for the treatment of mild to moderate AD [10]. Among these agents, donepezil interacts with both active-site gorge and PAS, in which the dimethoxyindanone part of donepezil binds to the PAS [11].

Structural development of AChE inhibitors resulted in introducing coumarin class of compounds such as ensaculine and AP2238 as anti-Alzheimer's agents (Fig. 1). Previous studies have demonstrated that coumarin motif can bind primarily to the PAS of AChE [12]. Accordingly, we have recently designed some novel coumarin-3-carboxamide derivatives linked to *N*-benzylpiperidine as potent AChE inhibitors [13]. Furthermore, we described 4-

* Corresponding author.
E-mail address: ashafiee@ams.ac.ir (A. Shafiee).

http://dx.doi.org/10.1016/j.ejmech.2014.05.056
0223-5234/

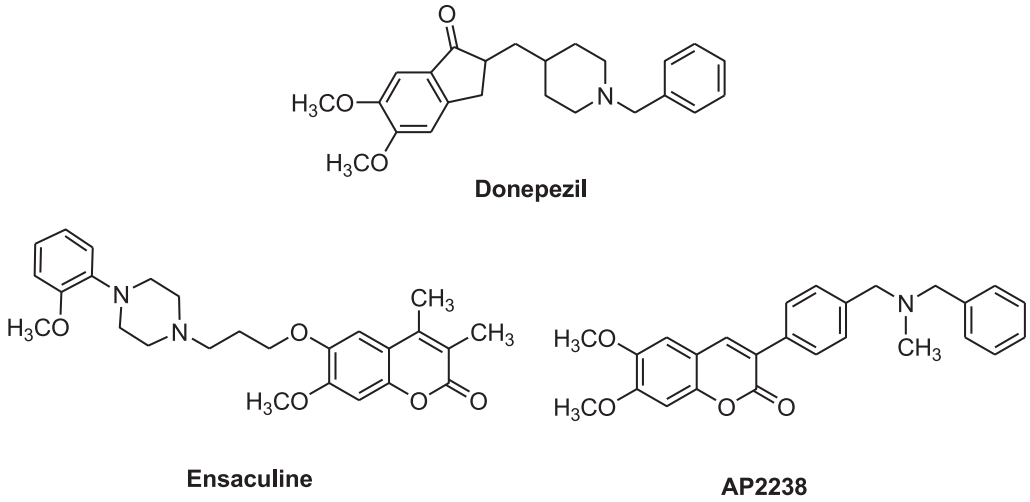

Fig. 1. Examples of known AChE inhibitors: donepezil as indanone derivative, and ensaculine and AP2238 as coumarin derivatives.

hydroxycoumarin derivatives in which an *N*-phenylpiperazine or *N*-benzylpiperidine moiety was connected with an alkoxy amide spacer to the coumarin scaffold. Particularly, *N*-(1-benzylpiperidin-4-yl)acetamide derivative displayed the highest AChE inhibitory activity [14]. In the search for finding new coumarin-based AChE inhibitors, we decided to displace the side chain from 4- to 7-position of coumarin core structure. Thus, in continues of our previous works on the synthesis of novel AChE inhibitors [13–15], we describe here synthesis and biological activity evaluation, as well as docking study of 2-(2-oxo-2*H*-chromen-7-yloxy)amides **4a**–**s**.

2. Chemistry

As illustrated in Scheme 1, the target compounds **4a**–**s** could be easily prepared starting from 7-hydroxycoumarins **1a,b**. 7-Hydroxycoumarin **1a** was commercially available and 4-methyl-7-hydroxycoumarin **1b** was prepared by using Pechmann condensation [16]. Compound **1** was converted to ethyl ester derivatives **2a**–**c** by *O*-alkylation with ethyl 2-bromoacetate or ethyl 4-bromobutanoate in the presence of K_2CO_3, in refluxing acetone. The esters **2** were hydrolyzed with aqueous solution of sodium hydroxide to afford the corresponding acids **3a**–**c**. Finally, different procedure were screened for the condensation of the carboxylic acids **3** with appropriate amines, such as application of dicyclohexylcarbodiimide (DCC), *N*-(3-dimethylaminopropyl)-*N*-ethylcarbodiimide hydrochloride (EDC) with hydroxybenzotriazole (HBT) and *N*-hydroxysuccinimide (NHS) in different solvents. Among these, the best result was obtained by EDC/HBT in acetonitrile.

3. Results and discussion

3.1. Pharmacology

3.1.1. Cholinesterase inhibitory activity

The cholinesterase inhibitory activity of synthesized compounds **4a**–**s** in comparison with standard drug donepezil was evaluated against AChE and BuChE enzymes and the results were expressed as IC_{50} values in Table 1. The tested compounds showed IC_{50}s ranging from 1.6 to 74 μM against AChE. Among them, benzylpiperidinylamino derivative **4r** exhibited the most potent inhibitory

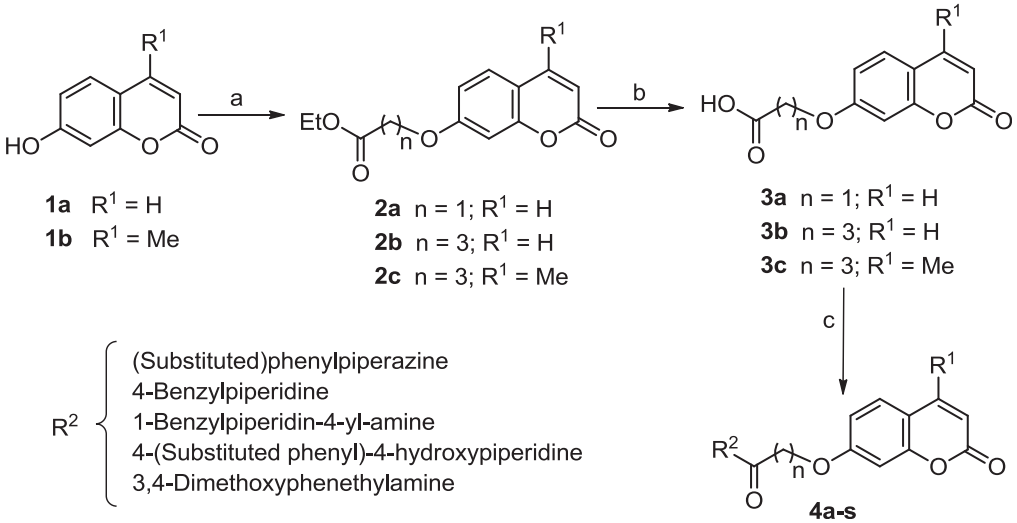

Scheme 1. Synthesis of compounds **4a**–**s**. *Reagents and conditions*: (a) Ethyl 2-bromoacetate or ethyl 4-bromobutanoate, K_2CO_3, acetone, reflux; (b) 10% NaOH (aq), reflux and then 6% HCl (aq); (c) appropriate amine, EDC, HBT, CH_3CN.

Table 1
The enzyme inhibitory activity (IC_{50}, μM) of the target compounds **4a**–**s** against AChE and BuChE.[a]

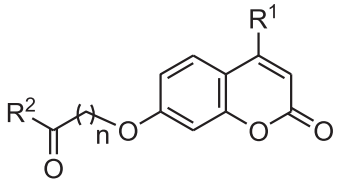

Compound	R^1	R^2	*n*	AChE	BuChE
4a	H	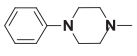	3	3.43 ± 0.19	120 ± 7
4b	H	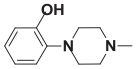	3	7 ± 0.38	280 ± 16
4c	H	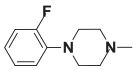	3	6.9 ± 0.37	15 ± 0.85
4d	H	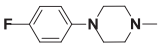	3	50 ± 2.8	75 ± 4.4
4e	H	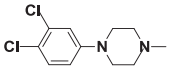	3	26 ± 1.77	80 ± 5.1
4f	H	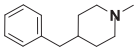	3	6.9 ± 0.4	387 ± 23
4g	H	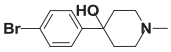	3	73 ± 4	180 ± 10
4h	CH_3	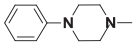	3	20.8 ± 1.8	68 ± 3.3
4i	CH_3	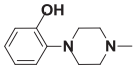	3	6.2 ± 0.18	184 ± 8.3
4j	CH_3	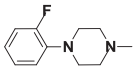	3	16.4 ± 0.98	29 ± 2.61
4k	CH_3	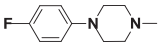	3	41.6 ± 2.3	24 ± 1.4
4l	CH_3	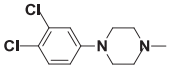	3	4.38 ± 0.24	250 ± 15
4m	CH_3	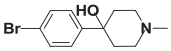	3	34.6 ± 2.26	141 ± 5.23
4n	H	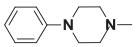	1	33 ± 1.8	50 ± 2.9
4o	H	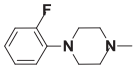	1	34.5 ± 1.9	86 ± 5
4p	H	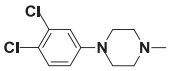	1	26.8 ± 1.5	120 ± 7
4q	H	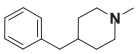	1	9.8 ± 0.54	46 ± 2.7
4r	H	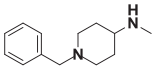	1	1.6 ± 0.088	42 ± 2.4
4s	H	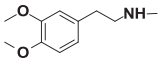	1	74 ± 4	163 ± 9.5
Donepezil	–	–	–	0.022 ± 0.001	7.3 ± 0.42

[a] Data are expressed as Mean ± SE (three independent experiments).

activity. However, compounds **4a**–**c**, **4f**, **4i**, **4l**, and **4q** showed good activity against AChE (IC_{50}s < 10 μM).

The obtained IC_{50} values of 4-phenylpiperazinyl derivative **4a**–**e** against AChE revealed that the substitution of phenyl ring by 2-OH, 2-F, 4-F and 3,4-Cl_2 diminished the activity (**4b**–**e** vs. **4a**). In contrast, in 4-methylcoumarin series **4h**–**l** containing 4-phenylpiperazinyl moiety, the 2-OH, 2-F and 3,4-Cl_2 groups increased the inhibitory activity towards AChE.

In the case of 4-unsubstituted coumarins with three carbons linker ($n = 3$), the (2-hydroxyphenyl)piperazine, (2-fluorophenyl) piperazine, and 4-benzylpiperidine derivatives (compounds **4b**, **4c** and **4f**, respectively) showed similar activities. While, among the 4-unsubstituted coumarins with $n = 1$, (1-benzylpiperidin-4-yl) amino moiety was more favorable than phenylpiperazine.

The comparison of 4-methylcoumarin derivatives **4h**–**m** and 4-unsubstituted coumarin analogs **4a**–**g** in terms of anti-AChE activity, revealed that the effect of methyl group at 4-position depended on the type of pendent group on the 7-position. For example, although the 4-methyl derivative **4l** was more potent than its unsubstituted analog **4e**, but 4-methyl derivative **4h** was less potent than corresponding analog **4a**.

As shown in Table 1, the length of side chain linker ($n = 1$ or 3) could affect the inhibitory activity. In phenylpiperazine derivatives, the activity of compound **4a** ($n = 3$) was higher than compound **4n** ($n = 1$). In addition, the anti-AChE activity of (2-fluorophenyl) piperazine derivative **4c** ($n = 3$) was superior than that of its analog **4o** bearing shorter linker ($n = 1$). Compounds **4e** and **4f** containing (3,4-dichlorophenyl)piperazine and benzylpiperidine were as potent as **4p** and **4q**, respectively. Thus, the effect of amidic linker depended on the type of substituted amine which attached to the linker. The survey of the IC_{50} values of (fluorophenyl)piperazine derivatives against AChE demonstrated that the 2-fluoro substituent is more favorable than the 4-fluoro one (**4c** vs. **4d** and **4j** vs. **4k**).

It should be noted that the most of target compounds have distal tertiary amine that would be protonated at the physiological pH. However, compounds **4f**, **4g**, **4m**, **4q** and **4s** contain only amidic nitrogen without distal amine. Interestingly amongst the latter compounds, 4-benzylpiperidine derivatives **4f** and **4q** showed good activities (IC_{50}s < 10 μM).

The IC_{50} values of compounds **4a**–**s** against BuChE were in the range of 15–387 μM, which were significantly higher than those of AChE. Among the tested compounds only (4-fluorophenyl)piperazine derivative **4k** showed more selective activity against BuChE. However, the (2-fluorophenyl)piperazine derivative **4c** was the most potent compound against BuChE. Notably, the effect of structural modifications on BuChE activity was the same as AChE. Nevertheless, the most potent compound against AChE (compound **4r**) was not the most active one against BuChE.

The coumarin nucleus has been extensively considered in the design of AChE inhibitors, resulted in introducing anti-Alzheimer's agents such as ensaculine and AP2238. In order to explore wide structure–activity relationships of coumarin derivatives, 3, 4, 6 or 7-substituted coumarins have been studied more extensively. Attachment of functionalized amine via an appropriate spacer to the mentioned positions of coumarin template is the typically explored modifications. Recently, we have synthesized a series of coumarin-3-carboxamide derivatives bearing *N*-benzylpiperidine side chain as potent AChE inhibitors [13]. Also, we have described 4-hydroxycoumarin derivatives containing *N*-phenylpiperazine or *N*-benzylpiperidine residues. Among them, *N*-(1-benzylpiperidin-4-yl)acetamide derivative displayed highest AChE inhibitory activity ($IC_{50} = 1.2$ μM) with 37-fold selectivity for AChE respect to the BuChE [14]. In the present work, we found that 7-hydroxycoumarin derivative **4r** containing *N*-(1-benzylpiperidin-4-yl)acetamide residue with IC_{50} value of 1.6 μM was the most potent compound

against AChE. These findings revealed that *N*-(1-benzylpiperidin-4-yl) substituent is a favorable scaffold to attaching to the 4- or 7-hydroxycoumarin scaffold via an acetamido linker.

3.1.2. Kinetic study of AChE inhibition

The most active compound **4r** was subjected to kinetic studies. For this purpose, the rate of the enzyme activity was measured at four different concentrations of compound **4r** (0, 0.64, 1.27 and 2.55 μM) using different concentration of the substrate acetylthiocholine (ATCh). In each case, the initial velocity was measured at different concentrations of the substrate (S), and the reciprocal of the initial velocity (1/v) was plotted against the reciprocal of [ATCh]. The double reciprocal (Lineweavere–Burk) plot showed a pattern of increasing slopes and increasing intercepts with higher inhibitor concentration (Fig. 2). This pattern indicates mixed-type inhibition of the enzyme by compound **4r**. The inhibitory constant (K_i) for the compound **4r** was calculated using secondary plot as depicted in Fig. 2 (K_i = 1.32 μM).

3.1.3. Ferric reducing antioxidant power (FRAP)

Ferric reducing antioxidant power (FRAP) assay was used to measure total antioxidant activity of the target compounds based on the method of Benzie and Strain [17]. In this method the compounds act as reductants in a redox-linked colorimetric method. In principle ferric tripyridyl triazine complex is reduced to ferrous form which has a deep blue color. The change of absorbance is measured at 585 nm. The antioxidant activity of the compounds is shown in Table 2. Compounds **4s** showed the highest antioxidant activity with FRAP value of 5.43. This compound was less effective than the standard antioxidants ascorbic acid and quercetin (FRAP value = 7.26 and 10.79 μmole Fe^{2+}/g, respectively). Moreover, compounds **4b**, **4i** and **4p** showed significant antioxidant activity.

3.1.4. Protective effect against H_2O_2-induced cell death in PC12 neurons

The neuroprotective activity of the compound **4r** against oxidative stress-induced cell death in differentiated PC12 cells was evaluated. The obtained data are shown in Fig. 3 in which the cell viability was determined in comparison with H_2O_2-treated group. The neuroprotective activity of the compound was evaluated at the concentrations of 1, 5, 10 μM. Moreover, quercetin was used as reference compound at the concentration of 5 μM. Compound **4r** exhibited no cytotoxic activity towards PC12 cells at the tested concentrations. Based on the results, H_2O_2 significantly reduced the cell viability to ~49% compared to the control. Pretreatment of PC12 cells with the compound **4r** significantly protected neurons against cell death in all used concentrations (P value < 0.001).

As expected for standard agent quercetin, the observed results from both FRAP assay (Table 2) and oxidative stress-induced cell death test in differentiated PC12 cells (Fig 3) revealed the high potential of quercetin as neuroprotective and antioxidant agent. In contrast, the selected compound **4r** which showed good protection against oxidative stress-induced cell death in differentiated PC12 cells was not an effective compound in FRAP assay. These results demonstrated that the protection mechanism of compound **4r** maybe different from that of quercetin.

3.2. Ligand-protein docking simulation

A molecular modeling study was performed to gain insight into the binding mode of target compounds to the AChE enzyme. For this purpose, all tested compounds **4a**–**s** were docked into the active site of the enzyme using Autodock Vina program and the best docked poses in terms of the free energy of binding were further analyzed to clarify interactions between ligands and the target enzyme. The results showed that all compounds were similarly oriented in the active site. In the case of the most active compound **4r** (Fig. 4), the ligand was well accommodated in the gorge of AChE active site so that the benzylpiperidin moiety was leaning toward the catalytic anionic subsite (CAS). Specifically, phenyl ring stacks against the Trp83 via T-shape (edge-to-face) π–π interaction and the piperidine ring that is located at the vicinity of the Phe329 and Phe330, formed a π-cation interaction. In this binding mode, the coumarin scaffold formed π-stacking with the aromatic ring of Trp278 in the PAS and its carbonyl group was hydrogen-bonded to Arg288. This binding mode is in agreement with mixed-mode inhibition pattern of **4r**, in which both CAS and PAS are occupied by the ligand.

4. Conclusion

We designed and synthesized 7-hydroxycoumarin derivatives connected by an amidic linker to the different amines such as (substituted)phenylpiperazine, 4-benzylpiperidine, 1-benzyl piperidin-4-yl-amino-, 4-(substituted phenyl)-4-hydroxypiperi dine. Most compounds showed remarkable inhibitory activity against AChE and BuChE. Among them, *N*-(1-benzylpiperidin-4-yl) acetamide derivative **4r** with IC_{50} value of 1.6 μM was the most

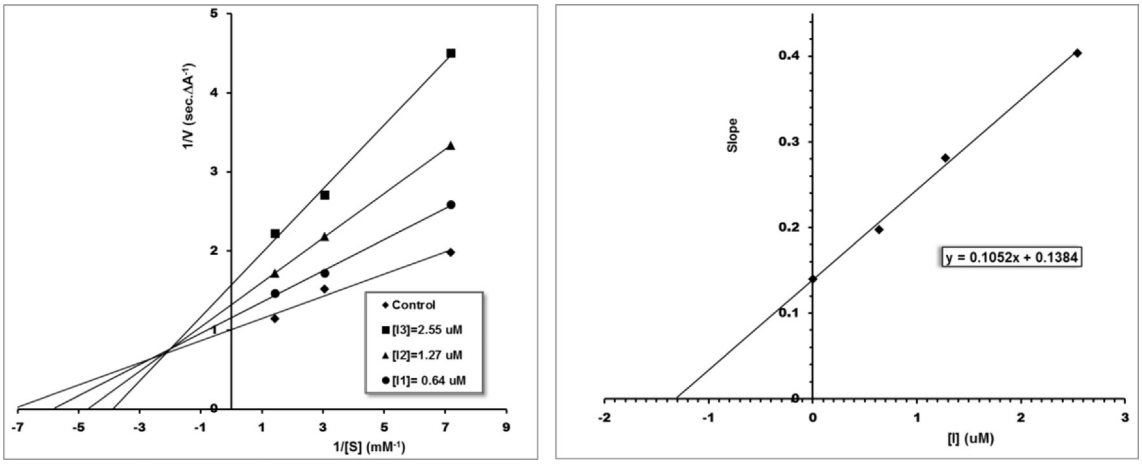

Fig. 2. Left: Lineweavere–Burk plot for the inhibition of AChE by compound **4r** at different concentrations of acetylthiocholine (ATCh), Right: Secondary plot of the enzyme for calculation of steady-state inhibition constant (K_i = 1.32 μM) of **4r**.

Table 2
The total antioxidant activity of the compounds **4a**–**s** determined by FRAP assay.

Compounds	FRAP values (μmole Fe^{2+}/g)
4a	1.13
4b	2.82
4c	0.15
4d	1.37
4e	0.78
4f	1.61
4g	0.03
4h	0.07
4i	2.01
4j	0.10
4k	0.08
4l	0.05
4m	0.06
4n	1.94
4o	0.07
4p	2.01
4q	0.05
4r	0.06
4s	5.43
Ascorbic acid	7.26
Quercetin	10.79

potent compound against AChE. The FRAP assay of synthesized compounds **4a**–**s** showed that some compounds had good antioxidant activity. Although the selected compound **4r** showed no significant antioxidant activity as evaluated by FRAP assay, but could significantly protect neurons against H_2O_2-induced cell death at low concentrations. The Kinetic study of AChE inhibition indicated a mixed-type inhibition of the enzyme by compound **4r**. The docking study of compound **4r** with AChE enzyme showed that both CAS and PAS are occupied by the ligand. These results make the prototype compounds **4** as promising cholinesterase inhibitors for further developments.

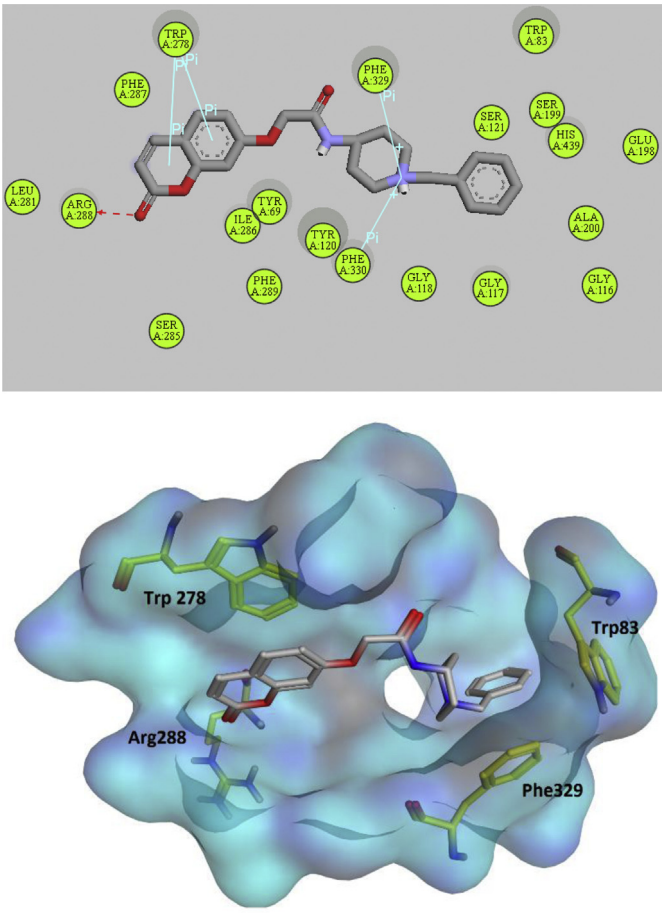

Fig. 4. The schematic 2D and 3D representations (top and bottom, respectively) of compound **4r**, docked in the active site of AChE.

5. Experimental

All starting materials, solvents and reagents were purchased from Sigma–Aldrich, Fluka, or Merck, and used without further purification. Melting points were measured on a Kofler hot stage apparatus and are uncorrected. The IR spectra were taken using Nicolet FT-IR Magna 550 spectrometer (KBr disks). ^{1}H NMR spectra were recorded on a Bruker 500 MHz NMR instrument. The chemical shifts (δ) and coupling constants (J) are expressed in parts per million (ppm) and Hertz (Hz), respectively. Mass spectra were obtained by using an HP (Agilent technologies) 5937 Mass Selective Detector. Elemental analyses were carried out with a Perkin–Elmer model 240-C apparatus. The results of elemental analyses (C, H, N) were within ±0.4% of the calculated values.

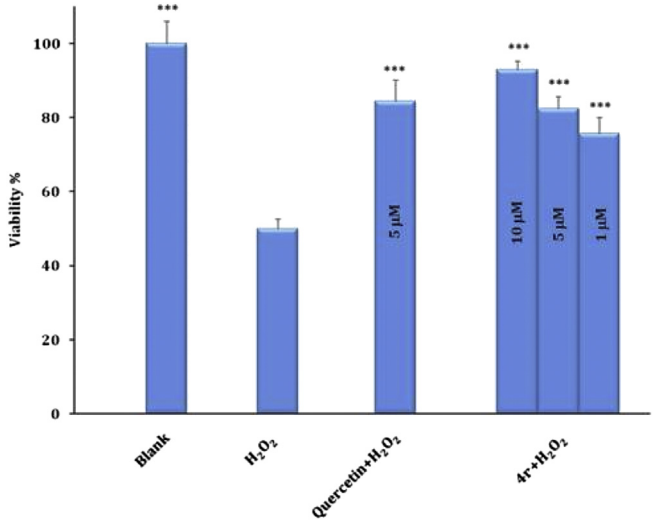

Fig. 3. Neuroprotective activity of compound **4r** against H_2O_2-induced cell death in differentiated PC12 cells (***$P < 0.001$).

5.1. General procedure for the synthesis of compounds *3a–c*

A mixture of 7-hydroxycoumarin (**1a**) or 4-methyl-7-hydroxycoumarin (**1b**) (5.0 mmol) and potassium carbonate (5.5 mmol) in acetone (5 ml) was stirred at room temperature for several minutes. Then, ethyl 2-bromoacetate or ethyl 4-bromobutanoate (5.2 mmol) was added dropwise to the mixture under argon atmosphere and the mixture was refluxed for 7–9 h. After completion of the reaction (monitored by TLC), the mixture was cooled to room temperature and diluted with water. The precipitated product **2** was collected by filtration and washed with water, and used without further purification. The crude product **2a**–**c** was dissolved in aqueous 10% NaOH (25 ml) and the solution was refluxed for 4 h. The reaction mixture was cooled and acidified with aqueous 6% HCl. The precipitated white solid was filtered off and subsequently washed with water to give compound **3**.

5.1.1. 2-((2-Oxo-2H-chromen-7-yl)oxy)acetic acid (*3a*)

Yield 96%; white crystal; mp 180–182 °C; IR (KBr, cm^{-1}) ν_{max}: 1746 and 1623 (C=O), 3362 (OH); ^{1}H NMR ($CDCl_3$, 500 MHz) δ 3.91

(s, 2H, CH_2O), 6.11 (d, 1H, H_3 coumarin, $J = 9.4$ Hz), 6.82–6.84 (m, 2H, $H_{6,8}$ coumarin), 7.27 (d, 1H, H_5 coumarin, $J = 8.3$ Hz), 7.52 (d, 1H, H_4 coumarin, $J = 9.4$ Hz). Anal. Calcd for $C_{11}H_8O_5$: C, 60.00; H, 3.66. Found: C, 60.32; H, 3.40.

*5.1.2. 4-(2-Oxo-2H-chromen-7-yloxy)butanoic acid (**3b**)*

Yield 98%; white crystal; mp 182–184 °C; IR (KBr, cm^{-1}) ν_{max}: 1725 and 1679 (C=O), 3083 (OH); ^1H NMR (DMSO-d_6, 500 MHz) δ 1.93–1.99 (m, 2H, $CH_2\underline{CH_2}CH_2$), 2.39 (t, 2H, CH_2C=O, $J = 7.3$ Hz), 4.09 (t, 2H, OCH_2, $J = 6.4$ Hz), 6.28 (d, 1H, H_3 coumarin, $J = 9.5$ Hz), 6.94 (dd, 1H, H_6 coumarin, $J = 2.5$ and 8.6 Hz), 6.97 (d, 1H, H_8 coumarin, $J = 2.5$ Hz), 7.61 (d, 1H, H_5 coumarin, $J = 8.6$ Hz), 7.98 (d, 1H, H_4 coumarin, $J = 9.5$ Hz). Anal. Calcd for $C_{13}H_{12}O_5$: C, 62.90; H, 4.87. Found: C, 63.24; H, 4.52.

*5.1.3. 4-(4-Methyl-2-oxo-2H-chromen-7-yloxy)butanoic acid (**3c**)*

Yield 97%; white crystal; mp 168–170 °C; IR (KBr, cm^{-1}) ν_{max}: 1736 and 1684 (C=O), 3457 (OH); ^1H NMR ($CDCl_3$, 500 MHz) δ 2.16–2.20 (m, 2H, $CH_2\underline{CH_2}CH_2$), 2.41 (s, 3H, CH_3), 2.62 (t, 2H, CH_2C=O, $J = 6.9$ Hz), 4.10 (t, 2H, OCH_2, $J = 5.7$ Hz), 6.15 (s, 1H, H_3 coumarin), 6.81 (s, 1H, H_8 coumarin), 6.86 (d, 1H, H_6 coumarin, $J = 8.6$ Hz), 7.50 (d, 1H, H_5 coumarin, $J = 8.6$ Hz). Anal. Calcd for $C_{14}H_{14}O_5$: C, 64.12; H, 5.38. Found: C, 64.37; H, 5.64.

*5.2. General procedure for the synthesis of compounds **4a–s***

Compound **3** (1.0 mmol), EDC (1.0 mmol) and HBT (1.0 mmol) were dispersed in dry acetonitrile (5 ml). The mixture was stirred at room temperature for 1 h and then appropriate amine (1.0 mmol) was added to the mixture. The mixture was stirred at room temperature for 24 h. After completion of the reaction (monitored by TLC), the solvent was evaporated and the residue was washed with saturated sodium carbonate. The resulting crude product was purified by crystallization from ethanol.

*5.2.1. 7-(4-Oxo-4-(4-phenylpiperazin-1-yl)butoxy)-2H-chromen-2-one (**4a**)*

Yield 87%, yellow crystal; mp 128–130 °C. IR (KBr, cm^{-1}) ν_{max}: 1721 and 1647 (C=O); ^1H NMR ($CDCl_3$, 500 MHz) δ 2.19–2.23 (m, 2H, $CH_2\underline{CH_2}CH_2$), 2.59 (t, 2H, CH_2C=O, $J = 6.7$ Hz), 3.16–3.18 (m, 4H, $2CH_2N$), 3.65–3.81 (m, 4H, $2CH_2N$), 4.12 (t, 2H, OCH_2, $J = 5.4$ Hz), 6.24 (d, 1H, H_3 coumarin, $J = 9.3$ Hz), 6.82–6.86 (m, 2H, H_8 coumarin and H phenyl), 6.90–6.93 (m, 3H, H_6 coumarin and 2H phenyl), 7.28 (t, 2H, 2H phenyl, $J = 7.3$ Hz), 7.37 (d, 1H, H_5 coumarin, $J = 8.4$ Hz), 7.63 (d, 1H, H_4 coumarin, $J = 9.3$ Hz). ^{13}C NMR ($CDCl_3$, 125 MHz) δ 24.0, 28.6, 41.0, 44.8, 48.9, 49.2, 67.2, 101.1, 112.0, 112.6, 116.1, 120.1, 128.3, 128.7, 142.9, 150.3, 155.3, 160.7, 161.6, 169.9. Anal. Calcd for $C_{23}H_{24}N_2O_4$: C, 70.39; H, 6.16; N, 7.14. Found: C, 70.76; H, 6.49; N, 7.48.

*5.2.2. 7-(4-(4-(2-Hydroxyphenyl)piperazin-1-yl)-4-oxobutoxy)-2H-chromen-2-one (**4b**)*

Yield 89%; yellow crystal; mp 151–153 °C; IR (KBr, cm^{-1}) ν_{max}: 1731 and 1624 (C=O), 3296 (OH); ^1H NMR ($CDCl_3$, 500 MHz) δ 2.20–2.24 (m, 2H, $CH_2\underline{CH_2}CH_2$), 2.61 (t, 2H, CH_2C=O, $J = 6.9$ Hz), 2.85–2.87 (m, 4H, $2CH_2N$), 3.67–3.81 (m, 4H, $2CH_2N$), 4.13 (t, 2H, OCH_2, $J = 5.6$ Hz), 6.26 (d, 1H, H_3 coumarin, $J = 9.4$ Hz), 6.83–6.91 (m, 4H, OH and 3H phenyl), 6.97 (d, 1H, H phenyl, $J = 7.8$ Hz), 7.07–7.13 (m, 2H, $H_{6,8}$ coumarin), 7.38 (d, 1H, H_5 coumarin, $J = 8.4$ Hz), 7.64 (d, 1H, H_4 coumarin, $J = 9.4$ Hz). ^{13}C NMR ($CDCl_3$, 125 MHz) δ 24.0, 28.6, 41.7, 45.5, 51.8, 52.2, 67.1, 101.1, 112.1, 112.6, 113.9, 119.7, 120.8, 126.4, 128.3, 137.6, 142.8, 150.7, 155.3, 160.7, 161.6, 170.0. Anal. Calcd for $C_{23}H_{24}N_2O_5$: C, 67.63; H, 5.92; N, 6.86. Found: C, 67.30; H, 6.30; N, 7.18.

*5.2.3. 7-(4-(4-(2-Fluorophenyl)piperazin-1-yl)-4-oxobutoxy)-2H-chromen-2-one (**4c**)*

Yield 85%; white crystal; mp 111–113 °C; IR (KBr, cm^{-1}) ν_{max}: 1723 and 1642 (C=O); ^1H NMR ($CDCl_3$, 500 MHz) δ 2.19–2.23 (m, 2H, $CH_2\underline{CH_2}CH_2$), 2.59 (t, 2H, CH_2C=O, $J = 6.6$ Hz), 3.05–3.07 (m, 4H, $2CH_2N$), 3.66–3.82 (m, 4H, $2CH_2N$), 4.12 (t, 2H, OCH_2, $J = 5.3$ Hz), 6.25 (d, 1H, H_3 coumarin, $J = 9.3$ Hz), 6.83 (s, 1H, H phenyl), 6.85 (d, 1H, H_6 coumarin, $J = 8.5$ Hz), 6.90–6.93 (m, 1H, H phenyl), 6.94–6.99 (m, 1H, H phenyl), 7.03–7.07 (m, 2H, H_8 coumarin and H phenyl), 7.37 (d, 1H, H_5 coumarin, $J = 8.5$ Hz), 7.63 (d, 1H, H_4 coumarin, $J = 9.3$ Hz). ^{13}C NMR ($CDCl_3$, 125 MHz) δ 24.0, 28.6, 41.2, 45.0, 49.8, 50.4, 67.2, 101.1, 112.1, 112.6, 115.6, 115.8, 118.6, 122.6, 122.7, 124.0, 128.3, 142.9, 154.2, 155.3, 160.7, 161.6, 169.9. Anal. Calcd for $C_{23}H_{23}FN_2O_4$: C, 67.31; H, 5.65; N, 6.83. Found: C, 67.68; H, 5.89; N, 6.37.

*5.2.4. 7-(4-(4-(4-Fluorophenyl)piperazin-1-yl)-4-oxobutoxy)-2H-chromen-2-one (**4d**)*

Yield 90%; yellow crystal; mp 138–140 °C; IR (KBr, cm^{-1}) ν_{max}: 1721 and 1652 (C=O); ^1H NMR ($CDCl_3$, 500 MHz) δ 2.19–2.23 (m, 2H, $CH_2\underline{CH_2}CH_2$), 2.59 (t, 2H, CH_2C=O, $J = 6.8$ Hz), 3.06–3.08 (m, 4H, $2CH_2N$), 3.65–3.79 (m, 4H, $2CH_2N$), 4.12 (t, 2H, OCH_2, $J = 5.5$ Hz), 6.25 (d, 1H, H_3 coumarin, $J = 9.4$ Hz), 6.82–6.91 (m, 4H, $H_{6,8}$ coumarin and 2H phenyl), 6.97 (m, 2H, 2H phenyl), 7.37 (d, 1H, H_5 coumarin, $J = 8.4$ Hz), 7.63 (d, 1H, H_4 coumarin, $J = 9.4$ Hz). ^{13}C NMR ($CDCl_3$, 125 MHz) δ 24.0, 28.6, 41.1, 44.9, 49.9, 50.2, 67.2, 101.1, 112.0, 112.6, 115.1, 115.3, 118.0, 118.1, 128.3, 142.8, 147.0, 155.3, 156.1, 158.0, 160.6, 161.6, 169.9. Anal. Calcd for $C_{23}H_{23}FN_2O_4$: C, 67.31; H, 5.65; N, 6.83. Found: C, 67.70; H, 5.84; N, 6.40.

*5.2.5. 7-(4-(4-(3,4-Dichlorophenyl)piperazin-1-yl)-4-oxobutoxy)-2H-chromen-2-one (**4e**)*

Yield 95%; white crystal; mp 139–141 °C; IR (KBr, cm^{-1}) ν_{max}: 1724 and 1650 (C=O); ^1H NMR ($CDCl_3$, 500 MHz) δ 2.19–2.23 (m, 2H, $CH_2\underline{CH_2}CH_2$), 2.59 (t, 2H, CH_2C=O, $J = 6.6$ Hz), 3.13–3.15 (m, 4H, $2CH_2N$), 3.64–3.79 (m, 4H, $2CH_2N$), 4.12 (t, 2H, OCH_2, $J = 5.3$ Hz), 6.25 (d, 1H, H_3 coumarin, $J = 9.3$ Hz), 6.74 (d, 1H, H phenyl, $J = 8.0$ Hz), 6.82 (s, 1H, H phenyl), 6.84 (d, 1H, H_6 coumarin, $J = 8.6$ Hz), 6.94 (s, 1H, H_8 coumarin), 7.29 (d, 1H, H phenyl, $J = 8.0$ Hz), 7.37 (d, 1H, H_5 coumarin, $J = 8.6$ Hz), 7.63 (d, 1H, H_4 coumarin, $J = 9.3$ Hz). ^{13}C NMR ($CDCl_3$, 125 MHz) δ 24.0, 28.6, 40.7, 44.5, 48.4, 48.5, 67.1, 101.1, 112.0, 112.6, 115.3, 117.3, 122.6, 128.3, 130.1, 132.4, 142.8, 149.7, 155.3, 160.6, 161.5, 169.9. Anal. Calcd for $C_{23}H_{22}Cl_2N_2O_4$: C, 59.88; H, 4.81; N, 6.07. Found: C, 60.21; H, 5.19; N, 6.35.

*5.2.6. 7-(4-(4-Benzylpiperidin-1-yl)-4-oxobutoxy)-2H-chromen-2-one (**4f**)*

Yield 85%; yellow crystal; mp 102–104 °C; IR (KBr, cm^{-1}) ν_{max}: 1720 and 1630 (C=O); ^1H NMR ($CDCl_3$, 500 MHz) δ 1.12–1.16 (m, 2H, $2\underline{CH}CH_2N$), 1.67–1.77 (m, 3H, CH piperidine and $2\underline{CH}CH_2N$), 2.15–2.19 (m, 2H, $CH_2\underline{CH_2}CH_2$), 2.51–2.57 (m, 5H, CH_2C=O, CHN and CH_2 benzyl), 2.91–2.98 (m, 2H, 2CHN), 3.85–3.87 (m, 1H, CHN), 4.10 (t, 2H, OCH_2, $J = 5.6$ Hz), 4.61–4.64 (m, 1H, CHN), 6.25 (d, 1H, H_3 coumarin, $J = 9.3$ Hz), 6.82 (s, 1H, H_8 coumarin), 6.85 (d, 1H, H_6 coumarin, $J = 8.4$ Hz), 7.13 (d, 1H, H phenyl, $J = 7.0$ Hz), 7.22 (t, 1H, H phenyl, $J = 7.0$ Hz), 7.26–7.31 (m, 2H, H phenyl), 7.37 (d, 1H, H_5 coumarin, $J = 8.4$ Hz), 7.64 (d, 1H, H_4 coumarin, $J = 9.3$ Hz). ^{13}C NMR ($CDCl_3$, 125 MHz) δ 24.1, 28.7, 31.3, 32.0, 37.7, 41.5, 42.4, 45.2, 67.3, 101.1, 112.0, 112.1, 112.5, 125.5, 127.8, 128.2, 128.5, 139.3, 142.9, 155.3, 160.7, 161.6, 169.6. Anal. Calcd for $C_{25}H_{27}NO_4$: C, 74.05; H, 6.71; N, 3.45. Found: C, 74.36; H, 6.42; N, 3.78.

*5.2.7. 7-(4-(4-(4-Bromophenyl)-4-hydroxypiperidin-1-yl)-4-oxobutoxy)-2H-chromen-2-one (**4g**)*

Yield 88%; white solid; mp 149–151 °C; IR (KBr, cm^{-1}) ν_{max}: 1725 and 1643 (C=O), 3450 (OH); ^1H NMR ($CDCl_3$, 500 MHz) δ 1.54–1.70 (m, 4H, $2CH_2$), 1.96–2.01 (m, 2H, $CH_2\underline{CH_2}CH_2$), 2.39 (t, 2H, CH_2C=O, J = 6.5 Hz), 2.87–2.93 (m, 1H, CHN), 3.36–3.60 (m, 2H, CH_2N), 3.92 (t, 2H, OCH_2, J = 5.5 Hz), 4.32–4.36 (m, 1H, CHN), 4.48 (s, 1H, OH), 6.03 (d, 1H, H_3 coumarin, J = 9.3 Hz), 6.62 (s, 1H, H_8 coumarin), 6.67 (d, 1H, H_6 coumarin, J = 8.3 Hz), 7.15 (d, 2H, H phenyl, J = 8.2 Hz), 7.21–7.27 (m, 3H, 2H phenyl and H_5 coumarin), 7.49 (d, 1H, H_4 coumarin, J = 9.3 Hz). ^{13}C NMR ($CDCl_3$, 125 MHz) δ 24.0, 28.4, 36.9, 37.2, 37.9, 41.1, 67.1, 69.7, 100.8, 111.8, 112.0, 112.2, 119.9, 126.0, 128.3, 130.4, 143.0, 147.2, 155.1, 160.5, 161.5, 169.5. Anal. Calcd for $C_{24}H_{24}BrNO_5$: C, 59.27; H, 4.97; N, 2.88. Found: C, 59.58; H, 4.62; N, 3.17.

*5.2.8. 4-Methyl-7-(4-oxo-4-(4-phenylpiperazin-1-yl)butoxy)-2H-chromen-2-one (**4h**)*

Yield 89%; white crystal; mp 143–145 °C; IR (KBr, cm^{-1}) ν_{max}: 1715 and 1644 (C=O); ^1H NMR ($CDCl_3$, 500 MHz) δ 2.19–2.23 (m, 2H, $CH_2\underline{CH_2}CH_2$), 2.40 (s, 3H, CH_3), 2.60 (t, 2H, CH_2C=O, J = 6.8 Hz), 3.15–3.17 (m, 4H, $2CH_2N$), 3.66–380 (m, 4H, $2CH_2N$), 4.12 (t, 2H, OCH_2, J = 5.6 Hz), 6.14 (s, 1H, H_3 coumarin), 6.83 (s, 1H, H_8 coumarin), 6.86–6.90 (m, 1H, H phenyl), 6.90–6.93 (m, 3H, H_6 coumarin and 2H phenyl), 7.28 (t, 2H, 2H phenyl, J = 7.3 Hz), 7.50 (d, 1H, H_5 coumarin, J = 8.7 Hz). ^{13}C NMR ($CDCl_3$, 125 MHz) δ 18.1, 24.0, 28.6, 41.0, 44.8, 48.9, 49.2, 67.1, 101.1, 111.5, 111.7, 113.1, 116.1, 120.1, 125.0, 128.7, 150.3, 152.0, 154.7, 160.8, 161.4, 169.9. Anal. Calcd for $C_{24}H_{26}N_2O_4$: C, 70.92; H, 6.45; N, 6.89. Found: C, 70.56; H, 6.18; N, 7.27.

*5.2.9. 7-(4-(4-(2-Hydroxyphenyl)piperazin-1-yl)-4-oxobutoxy)-4-methyl-2H-chromen-2-one (**4i**)*

Yield 91%; white crystal; mp 158–160 °C; IR (KBr, cm^{-1}) ν_{max}: 1725 and 1623 (C=O), 3326 (OH); ^1H NMR ($CDCl_3$, 500 MHz) δ 2.20–2.24 (m, 2H, $CH_2\underline{CH_2}CH_2$), 2.40 (s, 3H, CH_3), 2.61 (t, 2H, CH_2C=O, J = 6.9 Hz), 2.85–2.87 (m, 4H, $2CH_2N$), 3.67–3.81 (m, 4H, $2CH_2N$), 4.13 (t, 2H, OCH_2, J = 5.6 Hz), 6.14 (s, 1H, H_3 coumarin), 6.83–6.91 (m, 4H, OH and 3H phenyl), 6.97 (d, 1H, H phenyl, J = 7.8 Hz), 7.07–7.13 (m, 2H, $H_{6,8}$ coumarin), 7.50 (d, 1H, H_5 coumarin, J = 8.7 Hz). ^{13}C NMR ($CDCl_3$, 125 MHz) δ 18.1, 24.0, 28.6, 41.8, 45.5, 51.8, 52.2, 67.1, 101.1, 111.5, 111.7, 113.1, 113.9, 119.7, 120.8, 125.0, 126.4, 137.6, 142.8, 150.7, 152.0, 160.7, 161.4, 170.0. Anal. Calcd for $C_{24}H_{26}N_2O_5$: C, 68.23; H, 6.20; N, 6.63. Found: C, 67.95; H, 6.58; N, 6.29.

*5.2.10. 7-(4-(4-(2-Fluorophenyl)piperazin-1-yl)-4-oxobutoxy)-4-methyl-2H-chromen-2-one (**4j**)*

Yield 90%; white crystal; mp 123–125 °C; IR (KBr, cm^{-1}) ν_{max}: 1717 and 1654 (C=O); ^1H NMR (DMSO-d_6, 500 MHz) δ 1.97–2.00 (m, 2H, $CH_2\underline{CH_2}CH_2$), 2.36 (d, 3H, CH_3, J = 1.0 Hz), 2.52 (t, 2H, CH_2C=O, J = 7.2 Hz), 2.91–2.97 (m, 4H, $2CH_2N$), 3.58–3.62 (m, 4H, $2CH_2N$), 4.10 (t, 2H, OCH_2, J = 6.4 Hz), 6.17 (d, 1H, H_3 coumarin, J = 1.0 Hz), 6.92–7.00 (m, 4H, $H_{6,8}$ coumarin and 2H phenyl), 7.06–7.15 (m, 2H, 2H phenyl), 7.64 (d, 1H, H_5 coumarin, J = 9.0 Hz). ^{13}C NMR ($CDCl_3$, 125 MHz) δ 18.0, 24.1, 28.3, 41.0, 44.8, 50.0, 50.4, 67.6, 101.1, 111.0, 112.3, 113.0, 115.8, 116.0, 119.4, 122.7, 124.7, 126.3, 139.5, 153.3, 153.9, 154.7, 155.9, 160.1, 161.5, 170.0. Anal. Calcd for $C_{24}H_{25}FN_2O_4$: C, 67.91; H, 5.94; N, 6.60. Found: C, 67.68; H, 5.83; N, 6.35.

*5.2.11. 7-(4-(4-(4-Fluorophenyl)piperazin-1-yl)-4-oxobutoxy)-4-methyl-2H-chromen-2-one (**4k**)*

Yield 92%; yellow crystal; mp 162–164 °C; IR (KBr, cm^{-1}) ν_{max}: 1716 and 1653 (C=O); ^1H NMR ($CDCl_3$, 500 MHz) δ 2.19–2.23 (m, 2H, $CH_2\underline{CH_2}CH_2$), 2.39 (s, 3H, CH_3), 2.59 (t, 2H, CH_2C=O, J = 6.6 Hz), 3.06–3.08 (m, 4H, CH_2N), 3.65–3.79 (m, 4H, $2CH_2N$), 4.12 (t, 2H, OCH_2, J = 5.3 Hz), 6.13 (s, 1H, H_3 coumarin), 6.81 (s, 1H, H_8 coumarin), 6.86–6.88 (m, 3H, H_6 coumarin and 2H phenyl), 6.95–6.99 (m, 2H, 2H phenyl), 7.49 (d, 1H, H_5 coumarin, J = 8.6 Hz). ^{13}C NMR ($CDCl_3$, 125 MHz) δ 18.1, 24.0, 28.6, 41.1, 44.9, 49.9, 50.2, 67.1, 101.1, 111.4, 111.7, 113.1, 115.2, 115.3, 118.0, 118.1, 125.0, 147.0, 152.0, 154.7, 156.1, 158.0, 160.7, 161.4, 169.9. Anal. Calcd for $C_{24}H_{25}FN_2O_4$: C, 67.91; H, 5.94; N, 6.60. Found: C, 67.54; H, 6.29; N, 6.28.

*5.2.12. 7-(4-(4-(3,4-Dichlorophenyl)piperazin-1-yl)-4-oxobutoxy)-4-methyl-2H-chromen-2-one (**4l**)*

Yield 94%; white crystal; mp 143–145 °C; IR (KBr, cm^{-1}) ν_{max}: 1711 and 1649 (C=O); ^1H NMR ($CDCl_3$, 500 MHz) δ 2.19–2.23 (m, 2H, $CH_2\underline{CH_2}CH_2$), 2.40 (s, 3H, CH_3), 2.59 (t, 2H, CH_2C=O, J = 6.8 Hz), 3.13–3.15 (m, 4H, $2CH_2N$), 3.65–3.79 (m, 4H, $2CH_2N$), 4.12 (t, 2H, OCH_2, J = 5.5 Hz), 6.14 (s, 1H, H_3 coumarin), 6.74 (d, 1H, H phenyl, J = 8.0 Hz), 6.82 (s, 1H, H phenyl), 6.86 (d, 1H, H_6 coumarin, J = 8.6 Hz), 6.94 (s, 1H, H_8 coumarin), 7.30 (d, 1H, H phenyl, J = 8.0 Hz), 7.50 (d, 1H, H_5 coumarin, J = 8.6 Hz). ^{13}C NMR ($CDCl_3$, 125 MHz) δ 18.1, 24.0, 28.6, 40.7, 44.5, 48.4, 48.5, 67.0, 101.1, 111.5, 111.7, 113.1, 115.3, 117.3, 122.7, 125.0, 130.1, 132.4, 149.7, 151.9, 154.7, 160.7, 161.3, 170.0. Anal. Calcd for $C_{24}H_{24}Cl_2N_2O_4$: C, 60.64; H, 5.09; N, 5.89. Found: C, 60.31; H, 5.35; N, 6.29.

*5.2.13. 7-(4-(4-(4-Bromophenyl)-4-hydroxypiperidin-1-yl)-4-oxobutoxy)-4-methyl-2H-chromen-2-one (**4m**)*

Yield 88%; white solid; mp 149–151 °C; IR (KBr, cm^{-1}) ν_{max}: 1704 and 1638 (C=O), 3457 (OH); ^1H NMR (DMSO-d_6, 500 MHz) δ 1.56–1.84 (m, 4H, $2CH_2$), 1.96–2.01 (m, 2H, $CH_2\underline{CH_2}CH_2$), 2.39 (s, 3H, CH_3), 2.53–2.57 (m, 2H, CH_2CO), 2.89–2.95 (m, 1H, CHN), 3.38–3.41 (m, 1H, CHN), 3.77–3.80 (m, 1H, CHN), 4.11 (t, 2H, OCH_2, J = 5.5 Hz), 4.34–4.38 (m, 1H, CHN), 5.25 (s, 1H, OH), 6.21 (s, 1H, H_3 coumarin), 6.95–6.99 (m, 2H, $H_{6,8}$ coumarin), 7.39 (d, 2H, H phenyl, J = 7.9 Hz), 7.47 (d, 2H, H phenyl, J = 7.8 Hz), 7.67 (d, 1H, H_5 coumarin, J = 8.5 Hz). ^{13}C NMR (DMSO-d_6, 125 MHz) δ 18.1, 24.2, 28.2, 37.3, 37.9, 41.2, 67.9, 69.9, 101.1, 111.0, 112.3, 113.0, 119.4, 126.4, 127.1, 130.6, 148.7, 153.3, 154.7, 160.1, 161.6, 169.6. Anal. Calcd for $C_{25}H_{26}BrNO_5$: C, 60.01; H, 5.24; N, 2.80. Found: C, 59.78; H, 5.61; N, 2.44.

*5.2.14. 7-(2-Oxo-2-(4-phenylpiperazin-1-yl)ethoxy)-2H-chromen-2-one (**4n**)*

Yield 90%; white solid; mp 178–179 °C; IR (KBr, cm^{-1}) ν_{max}: 1728 and 1651 (C=O); ^1H NMR ($CDCl_3$, 500 MHz) δ 3.16–3.20 (m, 4H, $2CH_2N$), 3.70–3.80 (m, 4H, $2CH_2N$), 4.82 (s, 2H, CH_2O), 6.29 (d, 1H, H_3 coumarin, J = 9.3 Hz), 6.85–6.87 (m, 1H, H phenyl), 6.91–6.94 (m, 4H, $H_{6,8}$ coumarin and 2H phenyl), 7.27–7.30 (t, 2H, 2H phenyl, J = 7.4 Hz), 7.39 (d, 1H, H_5 coumarin, J = 8.3 Hz), 7.63 (d, 1H, H_4 coumarin, J = 9.3 Hz). ^{13}C NMR ($CDCl_3$, 125 MHz) δ 41.5, 44.6, 48.8, 49.3, 66.8, 95.3, 101.5, 112.0, 112.8, 113.2, 116.2, 120.2, 128.5, 128.7, 142.7, 150.2, 155.1, 160.4, 164.8. Anal. Calcd for $C_{21}H_{20}N_2O_4$: C, 69.22; H, 5.53; N, 7.69. Found: C, 68.94; H, 5.81; N, 7.83.

*5.2.15. 7-(2-(4-(2-Fluorophenyl)piperazin-1-yl)-2-oxoethoxy)-2H-chromen-2-one (**4o**)*

Yield 85%; white crystal; mp 198–199 °C; IR (KBr, cm^{-1}) ν_{max}: 1725 and 1651(C=O); ^1H NMR ($CDCl_3$, 80 MHz) δ 2.81–3.23 (m, 4H, $2CH_2N$), 3.42–3.81 (m, 4H, $2CH_2N$), 5.02 (s, 2H, OCH_2), 6.33 (d, 1H, H_3 coumarin, J = 9.4 Hz), 6.89–7.14 (m, 6H, 4H phenyl and $H_{6,8}$ coumarin), 7.65 (d, 1H, H_5 coumarin, J = 9.0 Hz), 7.93 (d, 1H, H_4 coumarin, J = 9.4 Hz). Anal. Calcd for $C_{21}H_{19}FN_2O_4$: C, 65.96; H, 5.01; N, 7.33. Found: C, 66.19; H, 5.29; N, 7.17.

*5.2.16. 7-(2-(4-(3,4-Dichlorophenyl)piperazin-1-yl)-2-oxoethoxy)-2H-chromen-2-one (**4p**)*

Yield 85%; white solid; mp 174–176 °C; IR (KBr, cm^{-1}) ν_{max}: 1731 and 1648 (C=O); ^1H NMR (DMSO-d_6, 500 MHz) δ 3.13–3.22 (m, 4H, $2CH_2N$), 3.60–3.61 (m, 4H, $2CH_2N$), 5.04 (s, 2H, CH_2O), 6.29 (d, 1H, H_3 coumarin, J = 9.5 Hz), 6.80–6.83 (m, 1H, H phenyl), 6.96–6.98 (m, 2H, H_6 coumarin and H phenyl), 7.01 (d, 1H, H_8 coumarin, J = 2.3 Hz), 7.22–7.26 (m, 1H, H phenyl), 7.62 (d, 1H, H_5 coumarin, J = 8.7 Hz), 7.99 (d, 1H, H_4 coumarin, J = 9.5 Hz). ^{13}C NMR (DMSO-d_6, 125 MHz) δ 41.0, 43.8, 48.2, 48.05, 65.9, 95.3, 101.4, 112.5, 112.8, 115.8, 119.3, 128.9, 129.2, 140.3, 144.2, 150.7, 155.1, 160.2, 161.2, 165.1. Anal. Calcd for $C_{21}H_{18}Cl_2N_2O_4$: C, 58.21; H, 4.19; N, 6.47. Found: C, 58.42; H, 4.09; N, 6.30.

*5.2.17. 7-(2-(4-Benzylpiperidin-1-yl)-2-oxoethoxy)-2H-chromen-2-one (**4q**)*

Yield 87%; yellow crystal; mp 101–103 °C. IR (KBr, cm^{-1}) ν_{max}: 1728 and 1620 (C=O); ^1H NMR ($CDCl_3$, 80 MHz) δ 1.10–1.41 (m, 2H, $2CHCH_2N$), 1.46–3.21 (m, 2H, $2CHCH_2N$), 3.21–3.40 (m, 5H, CH piperidine, 2CHN and CH_2 benzyl), 3.41–3.82 (m, 2H, 2CHN), 4.93 (m, 2H, OCH_2), 6.27 (d, 1H, H_3 coumarin, J = 9.4 Hz), 6.86–7.46 (m, 7H, 5H phenyl and $H_{6,8}$ coumarin), 7.55 (d, 1H, H_5 coumarin, J = 9.2 Hz), 7.92 (d, 1H, H_4 coumarin, J = 9.4 Hz). Anal. Calcd for $C_{23}H_{23}NO_4$: C, 73.19; H, 6.14; N, 3.71. Found: C, 72.89; H, 6.41; N, 3.82.

*5.2.18. N-(1-Benzylpiperidin-4-yl)-2-((2-oxo-2H-chromen-7-yl) oxy)acetamide (**4r**)*

Yield 82%; yellow crystal; mp 142–144 °C. IR (KBr, cm^{-1}) ν_{max}: 1735 and 1620 (C=O), 3258 (NH); ^1H NMR (DMSO-d_6, 80 MHz) δ 1.06–1.83 (m, 4H, $2CH_2CH_2N$), 2.75–3.19 (m, 4H, $2CH_2N$), 3.31–3.49 (m, 1H, CH piperidine), 3.44 (s, 2H, CH_2 benzyl), 4.57 (s, 2H, OCH_2), 6.32 (d, 1H, H_3 coumarin, J = 9.5 Hz), 6.82–7.48 (m, 7H, 5H phenyl and $H_{6,8}$ coumarin), 7.55 (d, 1H, H_5 coumarin, J = 9.3 Hz), 8.01 (d, 1H, H_4 coumarin, J = 9.5 Hz). Anal. Calcd for $C_{23}H_{24}N_2$: C, 70.39; H, 6.16; N, 7.14. Found: C, 70.68; H, 5.83; N, 7.39.

*5.2.19. N-(3,4-Dimethoxyphenethyl)-2-((2-oxo-2H-chromen-7-yl) oxy)acetamide (**4s**)*

Yield 84%; white crystal; mp 148–150 °C; IR (KBr, cm^{-1}) ν_{max}: 1734 and 1670 (C=O), 3364 (NH); ^1H NMR (DMSO-d_6, 500 MHz) δ 2.41–2.67 (m, 2H, CH_2), 3.12–3.46 (m, 2H, CH_2N), 3.64–3.65 (m, 6H, OCH_3), 4.58 (s, 2H, OCH_2), 6.31 (d, 1H, H_3 coumarin, J = 9.5 Hz), 6.69 (d, 1H, H phenyl, J = 8.5 Hz), 6.79 (s, 1H, H phenyl), 6.83 (d, 1H, H phenyl, J = 8.5 Hz), 6.95–6.97 (m, 2H, $H_{6,8}$ coumarin), 7.64 (d, 1H, H_5 coumarin, J = 8.3 Hz), 8.00 (d, 1H, H_4 coumarin, J = 9.5 Hz), 8.18–8.20 (m, 1H, NH). ^{13}C NMR (DMSO-d_6, 125 MHz) δ 30.6, 34.5, 55.2, 55.4, 67.1, 101.6, 111.7, 112.3, 112.6, 112.8, 120.3, 129.4, 131.5, 144.2, 147.1, 148.5, 155.1, 160.1, 160.7, 166.7. Anal. Calcd for $C_{21}H_{21}NO_6$: C, 65.79; H, 5.52; N, 3.65. Found: C, 65.95; H, 5.22; N, 3.86.

5.3. AChE and BuChE inhibition assay

Acetylcholinesterase (AChE, E.C. 3.1.1.7, Type V–S, lyophilized powder, from *electric eel*, 1000 unit), butyrylcholinesterase (BuChE, E.C. 3.1.1.8, from equine serum) and butyrylthiocholine iodide (BTCh) were provided from Sigma–Aldrich. 5,5′-Dithiobis-(2-nitrobenzoic acid) (DTNB), potassium dihydrogen phosphate, dipotassium hydrogen phosphate, potassium hydroxide, sodium hydrogen carbonate, and acetylthiocholine iodide (ATCh) were purchased from Fluka. The stock solutions of the target compounds were prepared in a mixture of DMSO (1 ml) and ethanol (9 ml) and diluted with 0.1 M KH_2PO_4/K_2HPO_4 buffer (pH = 8.0) to obtain final concentrations. 20 μl of substrate (acetylthiocholine iodide 0.075 M) was added to the test solution to obtain final concentration of 466 μM. All experiments were performed based on the previously described method [18]. Spectrophotometric measurements were performed on a UV Unico Double Beam Spectrophotometer. The same method was also taken for BuChE inhibition assay.

5.4. Ferric reducing antioxidant power (FRAP) assay

The FRAP assay was performed based on the method reported by Benzie and Strain [17] with slightly modification. 300 mM acetate buffer (3.1 g $C_2H_3NaO_2.3H_2O$ and 16 ml $C_2H_4O_2$), pH 3.6 and 10 mM TPTZ (2,4,6-tripyridyl-*s*-triazine) solution in 40 mM hydrochloric acid and 20 mM ferric chloride hexahydrate solution were mixed (FRAP solution). The temperature of the solution was raised to 37 °C before the assay. After that 300 μl of the compound stock solution was added the test solution was incubated for 15 min. Then, the change of absorbance was monitored at the 585 nm. Results are expressed in μmole ferrous/g dry mass of compounds according to the plotted standard curve of ferrous sulfate. Ascorbic acid was used as reference compound.

5.5. Cell culture, differentiation, and treatment conditions for cell viability assay

Rat undifferentiated PC12 cells were cultured in RPMI 1640 media with 10% FCS containing 100 units/ml penicillin and 100 μg/ml streptomycin (All from GIBCO, Grand Island, NY, USA). Cells were treated with trypsin and 10^4 cells were placed on each well of 96-well culture plates in RPMI 1640 media. For induction of neuronal differentiation, PC12 cells were cultured in serum-free media (RPMI 1640 media containing 100 units/ml penicillin and 100 μg/ml streptomycin) for 2 days, thereafter the medium changed to aforementioned serum free medium containing NGF (50 ng/ml, Sigma) and continued for 5 days until neurite outgrowth was observed by inverted microscope [19]. Differentiated PC12 cells were incubated with different concentrations (1, 5 and 10 μM) of the compounds for 3 h before treatment with H_2O_2 (300 μM). The occurrence of apoptosis was established after staining with DAPI, and cell viability was measured after 24 h by using the MTT assay as reported previously [20].

5.6. Docking studies

The crystal structure of *Torpedo californica* acetylcholinesterase (PDB entry code 1eve) in complex with E2020 was obtained from Protein Data Bank [21]. Then, the co-crystallized ligand and waters were removed from the protein. For docking experiments, ligand molecule was drawn using MarvineSketch 5.8.3, 2012, ChemAxon (http://www.chemaxon.com) and energy minimized to a minimum root mean standard deviation gradient of 0.100 using Chem3D Ultra. The structures were converted to 3D by means of Openbabel 2.3.1 [22]. Afterwards, the protein and optimized structures of ligands were converted to required pdbqt format using Autodock Tools 1.5.4 [23]. Docking simulations were performed with AutoDock vina 1.1.1 [24]. A box of 15 × 15 × 15 Å in *x*, *y* and *z* directions was used to cover all binding sites of the active site. The center of box was set to $x = 2.023$, $y = 63.295$, $z = 67.062$ (geometrical center of co-crystallized ligand). The exhaustiveness was set to 100 and the default settings were used for all other parameters. At the end of docking, the best dock poses with lowest binding free energies were further analyzed to find out possible interactions between the AChE and inhibitors. Molecular visualizations were carried out in DS Viewer Pro (Accelrys, Inc., San Diego, CA).

Acknowledgments

This work was supported by grants from the Research Council of Tehran University of Medical Sciences and the Iran National Science Foundation (INSF).

Appendix A. Supplementary data

Supplementary data related to this article can be found at http://dx.doi.org/10.1016/j.ejmech.2014.05.056.

References

[1] Alzheimer's Society: http://www.alzheimers.org.uk/.
[2] L. Fratiglioni, B. Winblad, E. von Strauss, Physiol. Behav. 92 (2007) 98–104.
[3] E. Scarpini, P. Scheltens, H. Feldman, Lancet Neurol. 2 (2003) 539–547.
[4] C. Holmes, D. Wilkinson, Adv. Psychiatr. Treat. 6 (2000) 193–200.
[5] P.N. Tariot, H. Federoff, J. Alzheimer Dis. Assoc. Disord. 17 (2003) 105–113.
[6] M.C. Dinamarca, D. Weinstein, O. Monasterio, N.C. Inestrosa, Biochemistry 50 (2011) 8127–8137.
[7] X.-C. He, S. Feng, Z.-F. Wang, Y. Shi, S. Zheng, Y. Xia, H. Jiang, X.-C. Tang, D. Bai, Bioorg. Med. Chem. 15 (2007) 1394–1408.
[8] N. Mishra, D. Sasmal, Bioorg. Med. Chem. Lett. 23 (2013) 702–705.
[9] A. Alvarez, R. Alarcón, C. Opazo, E.O. Campos, F.J. Muñoz, F.H. Calderón, F. Dajas, M.K. Gentry, B.P. Doctor, F.G. De Mello, J. Neurosci. 18 (1998) 3213–3223.
[10] R.A. Hansen, G. Gartlehner, A.P. Webb, L.C. Morgan, C.G. Moore, D.E. Jonas, Clin. Interv. Ag. 3 (2008) 211–225.
[11] S. Rizzo, M. Bartolini, L. Ceccarini, L. Piazzi, S. Gobbi, A. Cavalli, M. Recanatini, V. Andrisano, A. Rampa, Bioorg. Med. Chem. 18 (2010) 1749–1760.
[12] (a) P. Anand, B. Singh, N. Singh, Bioorg. Med. Chem. 20 (2012) 1175–1180; (b) Z. Radic, P. Taylor, J. Appl. Toxicol. 21 (2001) S13–S14; (c) V. Simeon-Rudolf, Z. Kovarik, Z. Radic, E. Reiner, Chem. Biol. Interact. 119–120 (1999) 119–128.
[13] A. Asadipour, M. Alipour, M. Jafari, M. Khoobi, S. Emami, H. Nadri, A. Sakhteman, A. Moradi, V. Sheibani, F. Homayouni Moghadam, A. Shafiee, A. Foroumadi, Eur. J. Med. Chem. 70 (2013) 623–630.
[14] S.F. Razavi, M. Khoobi, H. Nadri, A. Sakhteman, A. Moradi, S. Emami, A. Foroumadi, A. Shafiee, Eur. J. Med. Chem. 64 (2013) 252–259.
[15] (a) H. Akrami, B.F. Mirjalili, M. Khoobi, H. Nadri, A. Moradi, A. Sakhteman, S. Emami, A. Foroumadi, A. Shafiee, Eur. J. Med. Chem. (2014). in press; (b) M. Khoobi, M. Alipour, A. Moradi, A. Sakhteman, H. Nadri, S.F. Razavi, M. Ghandi, A. Foroumadi, A. Shafiee, Eur. J. Med. Chem. 68 (2013) 291–300; (c) M. Khoobi, M. Alipour, A. Sakhteman, H. Nadri, A. Moradi, M. Ghandi, S. Emami, A. Foroumadi, A. Shafiee, Eur. J. Med. Chem. 68 (2013) 260–269; (d) M. Alipour, M. Khoobi, H. Nadri, A. Sakhteman, A. Moradi, M. Ghandi, A. Foroumadi, A. Shafiee, Arch. Pharm. Chem. Life Sci. 346 (2013) 577–587; (e) M. Alipour, M. Khoobi, A. Foroumadi, H. Nadri, A. Moradi, A. Sakhteman, M. Ghandi, A. Shafiee, Bioorg. Med. Chem. 20 (2012) 7214–7222.
[16] B. Kiskhan, Y. Yagci, J. Polym. Sci. 45 (2007) 1670–1676.
[17] F.F. Benzie, J.J. Strain, Methods Enzymol. 299 (1999) 15–23.
[18] H. Nadri, M. Pirali-Hamedani, A. Moradi, A. Sakhteman, A. Vahidi, V. Sheibani, A. Asadipour, N. Hosseinzadeh, M. Abdollahi, A. Shafiee, A. Foroumadi, Daru J. Pharm. Sci. 21 (2013) 15.
[19] S.H. Koh, S.H. Kim, H. Kwon, Y. Park, K.S. Kim, C.W. Song, J. Kim, M.H. Kim, H.J. Yu, J.S. Henkel, H.K. Jung, Brain Res. Mol. Brain Res. 118 (2003) 72–81.
[20] D. Zsolt, A. Juhász, M. Gálfi, K. Soós, R. Papp, D. Zádori, B. Penke, Brain Res. Bull. 62 (2003) 223–229.
[21] RCSB Protein Data Bank, 2012. http://www.rcsb.org/pdb/home/home.do.
[22] N.M. O'Boyle, M. Banck, C.A. James, C. Morley, T. Vandermeersch, G.R. Hutchison, J. Cheminform. 3 (2011) 33.
[23] M.F. Sanner, J. Mol. Graph. Model 17 (1999) 57–61.
[24] O. Trott, A.J. Olson, J. Comput. Chem. 31 (2010) 455–461.